

# The Poincaré map and the method of averaging: A comparative study

John D. Hadjidemetriou  
Department of Physics,  
University of Thessaloniki, Thessaloniki, Greece

## 1 Introduction

There are two different ways to study the properties and the evolution of a dynamical system: The *Poincaré map on a surface of section* and the *method of averaging*. The Poincaré map is based mainly on numerical integrations, while the method of averaging is an analytical tool (or, in some cases a semi-analytical tool), followed in many cases by numerical integrations. Each method has its advantages and disadvantages. The Poincaré map describes *exactly* the dynamical system, but is subject to the limitations of the numerical work, mainly the accuracy of the numerical integrations for long time intervals. The method of averaging is based on a perturbation theory, by making use of series expansions which are truncated to a certain order. This introduces errors, and in some cases the dynamical model of the truncated, averaged, model is different from the original model. This is due either to the fact that the order of the truncation is low, or, most likely, to the fact that the perturbation series do not converge, being asymptotic series. This latter case is the rule, since almost all dynamical systems are non-integrable. However, the perturbation method is still valid in these cases, not in the whole phase space, but only in regions where the system is not chaotic.

In many studies of the dynamics of a system, either the Poincaré map or the averaging method are used. We believe that a combination of these two methods will give very useful results. As we mentioned, the Poincaré map is an exact method, which means that the topology of the phase space of the Poincaré map is identical with the topology of the phase space of the original, non-averaged system. It is clear that the topology of the phase space of the Poincaré map is determined by the fixed points (periodic orbits of the non-averaged system) and their stability properties. In order for the averaged system to be realistic, its phase space must have the same topology as the Poincaré map, which implies that it must have the same fixed points, with the same stability properties, as the Poincaré map. This is a simple *necessary* criterion to check the validity of the averaged model.

In what follows we shall present the method of the Poincaré map on a surface of section and the method of averaging, for a *nearly integrable dynamical system*. Next, we shall apply these two methods to a simple dynamical model, and we shall explain the similarities and the differences between them. As we will see in the next sections, these two methods give similar results, not only qualitatively, but also quantitatively, only when the perturbation is small and the system behaves as integrable, i.e. its phase space is ordered. However, for a larger perturbation, where the system develops chaotic motion, the method of averaging fails.

## 2 The Poincaré map for nearly integrable dynamical systems

Let us consider a Hamiltonian system

$$H = H_0(q_1, q_2, p_1, p_2) + \varepsilon H_1(q_1, q_2, p_1, p_2), \quad (1)$$

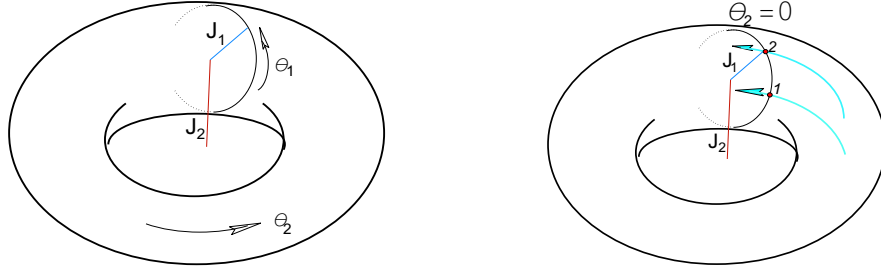


Figure 1: (a) The motion of the unperturbed system (5) on the 2-torus. (b) The mapping on the 2-torus at  $\theta_2 = 0$ .

where the Hamiltonian

$$H_0(q_1, q_2, p_1, p_2) \quad (2)$$

is integrable. We make a canonical change of variables, to action-angle variables of the integrable Hamiltonian (Lichtenberg and Liebermann, 1983)

$$q, p \rightarrow \theta, J \quad (3)$$

and the new Hamiltonian takes the form

$$H = H_0(J_1, J_2) + \varepsilon H_1(J_1, J_2, \theta_1, \theta_2). \quad (4)$$

### The unperturbed system

We start the study with the unperturbed problem, defined by the Hamiltonian

$$H = H_0(J_1, J_2). \quad (5)$$

The differential equations of motion are

$$\begin{aligned} \dot{\theta}_1 &= \frac{\partial H_0}{\partial J_1} = n_1, & \dot{J}_1 &= -\frac{\partial H_0}{\partial \theta_1}, \\ \dot{\theta}_2 &= \frac{\partial H_0}{\partial J_2} = n_2, & \dot{J}_2 &= -\frac{\partial H_0}{\partial \theta_2}, \end{aligned} \quad (6)$$

and the solution is

$$J_1 = J_{10}, \quad J_2 = J_{20}, \quad n_1 = \text{const.}, \quad n_2 = \text{const.} \quad (7)$$

This means that the motion is on a 2-torus, with radii  $J_1$  and  $J_2$  and angles  $\theta_1$  and  $\theta_2$ , as shown in Figure 1a.

We define now the *Poincaré map* on the surface of section

$$H_0(J_1, J_2) = h, \quad \theta_2 = 0, \quad \text{mod}(2\pi) \quad (8)$$

as shown in Figure 1b.

The mapping equations are given by

$$\begin{aligned} J_1 &\rightarrow J_1, \\ \theta_1 &\rightarrow \theta_1 + 2\pi \frac{n_1}{n_2}. \end{aligned} \quad (9)$$

From the differential equations (6) we easily see that the frequencies  $n_1$  and  $n_2$  are functions of  $J_1$  and  $J_2$ . Since however  $H_0(J_1, J_2) = h$ , the ratio  $n_1/n_2$  is a function of  $J_1$  and the energy  $h$ ,

which is a parameter of the mapping (9). Consequently, the mapping (9) is a *twist map*. Note that the time for one revolution along the angle  $\theta_2$  is

$$T = \frac{2\pi}{n_2}. \quad (10)$$

The Poincaré map (9) is a symplectic map and is generated by the generating function

$$F = J_{1,n+1}\theta_{1,n} + G_0(J_{1,n+1}), \quad (11)$$

through the relations

$$J_{1,n} = \frac{\partial F}{\partial \theta_{1,n}}, \quad \theta_{1,n+1} = \frac{\partial F}{\partial J_{1,n+1}}, \quad (12)$$

where the function  $G_0$  is obtained from

$$\frac{\partial G_0}{\partial J_{1,n+1}} = 2\pi \frac{n_1}{n_2} = 2\pi \frac{\partial H_0 / \partial J_1}{\partial H_0 / \partial J_2}. \quad (13)$$

Using the relation  $H_0(J_1, J_2) = h$ , we obtain

$$2\pi \frac{\partial H_0 / \partial J_1}{\partial H_0 / \partial J_2} = f(J_1; h), \quad (14)$$

where  $f(J_1; h)$  is a function of  $J_1$  and  $h$ , and finally we find that the function  $G_0$  is given by

$$G_0 = \int f(J_1; h) dJ_1. \quad (15)$$

We can easily see that the mapping (9) has the energy  $h$  as a parameter.

The mapping (9) can be expressed in the Poincaré variables

$$X_1 = \sqrt{2J_1} \cos \theta_1, \quad Y_1 = \sqrt{2J_1} \sin \theta_1, \quad (16)$$

which are also canonical variables. The Poincaré map in the variables (16) is shown in Figure 2, in the space  $X_1 Y_1$ . We see that the successive points of the mapping corresponding to the initial conditions

$$J_1 = J_{10}, \quad \theta_1 = \theta_{10}$$

are on the circle

$$\sqrt{2J_1} = \text{constant}$$

and the angle between two successive points is

$$\Delta\theta_1 = 2\pi \frac{n_1}{n_2} = \text{constant},$$

as shown in Figure 2. Note that the angle  $\Delta\theta_1$  depends on  $J_1$  (and the energy  $h$ ), implying that it is a twist map. The circle  $\sqrt{2J_1} = \text{constant}$  is mapped to itself, and for this reason it is called an *invariant curve (circle)*. If the ratio  $n_1/n_2$  is not rational, the consecutive points of the map are dense on the invariant circle. If however  $n_1/n_2 = p/q = \text{rational}$ , *each point* on the circle is an *invariant point*, in general multiple (it comes to the initial point after several repetitions of the map).

### The perturbed problem

Let us consider now a perturbed twist map, obtained from the generating function (11) by adding a perturbation term,

$$F = J_{1,n+1}\theta_{1,n} + G_0(J_{1,n+1}) + \varepsilon G_1(\theta_{1,n}, J_{1,n+1}), \quad (17)$$

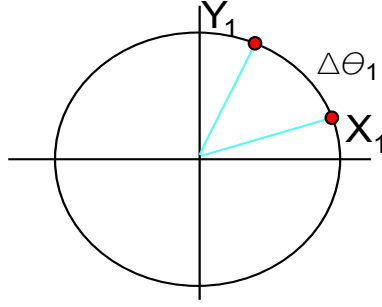


Figure 2: The mapping (9) in the Poincaré variables  $X_1 = \sqrt{2J_1} \cos \theta_1$ ,  $Y_1 = \sqrt{2J_1} \sin \theta_1$ . The radius of the invariant circle is equal to  $\sqrt{2J_1}$ .

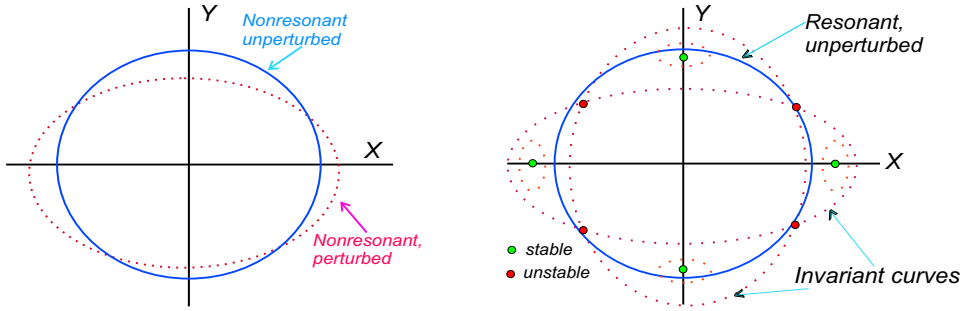


Figure 3: (a) A circular unperturbed irrational invariant circle survives the perturbation and becomes a nearly circular invariant curve. (b) The infinite fixed points of a rational invariant curve disappear and only a finite, even, number survive the perturbation, half stable and half unstable.

where  $\varepsilon$  is a small parameter. The perturbed twist map, obtained by making use of the relations (12), is given by

$$\left. \begin{aligned} J_1 &\rightarrow J_1 - \varepsilon \frac{\partial G_1}{\partial \theta_{1,n}} \\ \theta_1 &\rightarrow \theta_1 + 2\pi \frac{n_1}{n_2} + \varepsilon \frac{\partial G_1}{\partial J_{1,n+1}} \end{aligned} \right\}. \quad (18)$$

This mapping is symplectic and represents the Poincaré map of the perturbed system (4), at the surface of section  $\theta_2 = 0$ , for a suitable function  $G_1$ , corresponding to the perturbation  $\varepsilon H_1(J_1, J_2, \theta_1, \theta_2)$  in the Hamiltonian (4). Note that a basic property of the Poincaré map is its symplectic property (Hadjidemetriou 1998).

We ask now the question what happens to the invariant circles of the unperturbed map (9) that we mentioned above. There are two different cases: The ratio  $n_1/n_2$  to be irrational, or to be rational. If it is irrational, then for sufficiently small perturbation  $\varepsilon$ , the KAM theorem applies (Arnold 1974, Lichtenberg and Liebermann 1983). This means that the circular invariant curves survive the perturbation, as closed nearly circular invariant curves. This is shown graphically in Figure 3a.

If however the ratio  $n_1/n_2$  is rational, then the Poincaré-Birkhoff fixed-point theorem applies (Arnold and Avez 1968, Lichtenberg and Liebermann 1983), which means that out of the infinite set of fixed points on the unperturbed invariant circle, only a finite even number of fixed points survives, half of them stable and half unstable. In most cases only two fixed points survive, which are multiple, in general, one stable and the other unstable. Around a stable fixed point we have closed invariant curves, while at the unstable fixed points we have a hyperbolic map.

This is shown graphically in Figure 3b, where an example of a quadruple fixed point is presented. We remark that a rational invariant curve is usually related to resonances.

Relation between the Poincaré map and the motion on the torus.

From the above one can see that for a sufficiently small perturbation  $\varepsilon$  the torus of the unperturbed system, shown in Figure 1a, is transformed to a perturbed torus, which means that the motion is still bounded. The *fixed points* of the perturbed map (18) correspond to *periodic motion*. On the other hand, the motion on the Poincaré map which lies on an irrational invariant curve, corresponds to quasi periodic motion on the perturbed torus.

### 3 The method of averaging

We shall present the method of averaging in the case of a nearly integrable dynamical system, described by the Hamiltonian

$$H = H_0(q_1, q_2, p_1, p_2) + \varepsilon H_1(q_1, q_2, p_1, p_2), \quad (19)$$

where  $H = H_0(q_1, q_2, p_1, p_2)$  is the integrable part. We perform a canonical change of variables, to action-angle variables of the integral Hamiltonian,

$$q, p \rightarrow \theta, J \quad (20)$$

and the new Hamiltonian takes the form

$$H = H_0(J_1, J_2) + \varepsilon H_1(J_1, J_2, \theta_1, \theta_2). \quad (21)$$

As we mentioned in the previous section, the motion of the integrable system takes place on a 2-torus, with constant radii  $J_1, J_2$  and constant frequencies  $n_1, n_2$ , as shown in Figure 1a.

In order to apply the method of averaging, we must have a ‘fast’ and a ‘slow’ angle. This can be achieved close to a resonance, where the ratio of the frequencies is a rational number,  $n_1/n_2 = \text{rational}$ . As we shall show in the following, by an example, we can perform a new canonical change of variables, to *resonance variables*, where one angle is a ‘fast’ angle and the other a ‘slow’ ‘angle’.

Let us consider, as an example to present the method of averaging, a Hamiltonian system with two degrees of freedom, in the variables  $\theta_1, \theta_2, J_1, J_2$ , defined by the Hamiltonian

$$H = H_0(J_1, J_2) + \varepsilon H_{11}(J_1, J_2) \cos(2\theta_1 - \theta_2) + \varepsilon H_{rs}(J_1, J_2) \cos(r\theta_1 - s\theta_2), \quad (22)$$

where  $\varepsilon$  is a small parameter. The frequencies of the system are

$$n_1 = n_{10} + \varepsilon \frac{\partial H_{11}}{\partial J_1} \cos(2\theta_1 - \theta_2) + \varepsilon \frac{\partial H_{rs}}{\partial J_1} \cos(r\theta_1 - s\theta_2), \quad n_{10} = \frac{\partial H_0}{\partial J_1}, \quad (23)$$

and

$$n_2 = n_{20} + \varepsilon \frac{\partial H_{11}}{\partial J_2} \cos(2\theta_1 - \theta_2) + \varepsilon \frac{\partial H_{rs}}{\partial J_2} \cos(r\theta_1 - s\theta_2), \quad n_{20} = \frac{\partial H_0}{\partial J_2}, \quad (24)$$

where  $n_{10}, n_{20}$  are the unperturbed frequencies.

We consider initial conditions close to the region corresponding to the resonance  $n_{10}/n_{20} = s/r$ . The relation

$$\frac{\partial H_0 / \partial J_1}{\partial H_0 / \partial J_2} = \frac{s}{r} \quad (25)$$

defines a curve in the space  $J_1 J_2$ , which gives the initial conditions of the exact  $s/r$  resonance, for any value of the angles  $\theta_1, \theta_2$ .

Resonance angles at the  $s/r$  resonance

We perform now a canonical change of variables, to resonance variables,

$$J, \theta \rightarrow \hat{J}, \hat{\theta}, \quad (26)$$

by making use of the generating function

$$F = (\theta_1 - \frac{s}{r}\theta_2)\hat{J}_1 + \theta_2\hat{J}_2, \quad (27)$$

through the transformation equations (12). The relation between the old and the new variables is

$$\left. \begin{aligned} \hat{J}_1 &= J_1, & \hat{J}_2 &= \frac{s}{r}J_1 + J_2 \\ \hat{\theta}_1 &= \theta_1 - \frac{s}{r}\theta_2, & \hat{\theta}_2 &= \theta_2 \end{aligned} \right\}, \quad (28)$$

and we see that the angle  $\hat{\theta}_1$  is a ‘slow’ angle close to the  $s/r$  resonance,

$$\dot{\theta}_1/\dot{\theta}_2 \approx s/r \rightarrow \dot{\hat{\theta}} \approx 0.$$

The new Hamiltonian, in the resonance variables, is

$$\begin{aligned} \hat{H} &= \hat{H}_0(\hat{J}_1, \hat{J}_2) + \varepsilon\hat{H}_{11}(\hat{J}_1, \hat{J}_2) \cos(2\hat{\theta}_1 + \frac{2s-r}{r}\hat{\theta}_2) + \\ &\varepsilon\hat{H}_{rs}(\hat{J}_1, \hat{J}_2) \cos(r\hat{\theta}_1), \end{aligned} \quad (29)$$

where

$$\hat{H}_0(\hat{J}_1, \hat{J}_2) = H_0(\hat{J}_1, -\frac{s}{r}\hat{J}_1 + \hat{J}_2), \quad (30)$$

and similar relations for  $\hat{H}_{11}(\hat{J}_1, \hat{J}_2)$  and  $\hat{H}_{rs}(\hat{J}_1, \hat{J}_2)$ . The unperturbed frequencies in the new variables are

$$\hat{n}_1 = \partial\hat{H}_0/\partial\hat{J}_1 = n_1 - (s/r)n_2, \quad (31)$$

$$\hat{n}_2 = \partial\hat{H}_0/\partial\hat{J}_2 = n_2.$$

Note that since we are close to the  $s/r$  resonance, we have  $n_1/n_2 \approx s/r$  and consequently the angle  $\hat{\theta}_1$  is a ‘slow’ angle, because

$$\hat{n}_1 = n_1 - (s/r)n_2 \approx 0, \quad \hat{n}_1 = d\hat{\theta}_1/dt,$$

while  $\hat{\theta}_2$  is a ‘fast’ angle, since  $\hat{n}_2 = n_2$ . In this way, going to resonance variables, we created a ‘fast’ and a ‘slow’ angle. The system has, evidently, two degrees of freedom.

The averaged Hamiltonian at the  $s/r$  resonance

We continue now by a new canonical change of variables,

$$\hat{J}, \hat{\theta} \rightarrow \bar{J}, \bar{\theta}$$

in order to make the ‘fast’ angle ignorable. This can be achieved by the generating function

$$F = \bar{J}_1\hat{\theta}_1 + \bar{J}_2\hat{\theta}_2 + \varepsilon S(\bar{J}_1, \bar{J}_2, \hat{\theta}_1, \hat{\theta}_2), \quad (32)$$

where the term  $\bar{J}_1 \hat{\theta}_1 + \bar{J}_2 \hat{\theta}_2$  corresponds to the identity transformation and the function  $S(\bar{J}_1, \bar{J}_2, \hat{\theta}_1, \hat{\theta}_2)$  is to be determined. The new canonical transformation is

$$\hat{J}_i = \bar{J}_i + \varepsilon \frac{\partial S}{\partial \hat{\theta}_i}, \quad \hat{\theta}_i = \bar{\theta}_i - \varepsilon \frac{\partial S}{\partial \bar{J}_i}, \quad (i = 1, 2) \quad (33)$$

which is close to the identity transformation.

The Hamiltonian in the variables  $\bar{J}, \bar{\theta}$  is

$$\begin{aligned} \bar{H} &= \hat{H}_0(\bar{J}_1, \bar{J}_2) + \varepsilon \frac{\partial \hat{H}_0}{\partial \bar{J}_1} \frac{\partial S}{\partial \hat{\theta}_1} + \varepsilon \langle \hat{H}_1 \rangle_{\theta_2} + \\ &\varepsilon \left[ \frac{\partial \hat{H}_0}{\partial \bar{J}_2} \frac{\partial S}{\partial \hat{\theta}_2} + \{ \hat{H}_1 \} \right] + O(\varepsilon^2). \end{aligned} \quad (34)$$

In this expression the term

$$\langle \hat{H}_1 \rangle_{\theta_2} = \hat{H}_{rs} \cos(r\bar{\theta}_1) \quad (35)$$

is the mean value of  $\hat{H}_1$  with respect to  $\theta_2$ , obtained from

$$\begin{aligned} \hat{H}_1 &= \varepsilon \hat{H}_{11}(\hat{J}_1, \hat{J}_2) \cos(\hat{\theta}_1 - \frac{s-r}{r} \hat{\theta}_2) + \\ &\varepsilon \hat{H}_{rs}(\hat{J}_1, \hat{J}_2) \cos(r\hat{\theta}_1), \end{aligned}$$

and

$$\{ \hat{H}_1 \} = \hat{H}_{11} \cos(\bar{\theta}_1 + \frac{2s-r}{r} \bar{\theta}_2).$$

We shall keep first order terms in  $\varepsilon$  only in this Hamiltonian. We note that

$$\varepsilon \frac{\partial \hat{H}_0}{\partial \bar{J}_1} \frac{\partial S}{\partial \hat{\theta}_1}$$

is of higher order, since

$$\frac{\partial \hat{H}_0}{\partial \bar{J}_1} = \hat{n}_1 \simeq 0.$$

So, if we ignore this term, the Hamiltonian (34) takes the form

$$\bar{H} = \hat{H}_0(\bar{J}_1, \bar{J}_2) + \varepsilon \langle \hat{H}_1 \rangle_{\theta_2} + \varepsilon \left[ \frac{\partial \hat{H}_0}{\partial \bar{J}_2} \frac{\partial S}{\partial \hat{\theta}_2} + \{ \hat{H}_1 \} \right] + O(\varepsilon^2). \quad (36)$$

We select now the function  $S(\bar{J}_1, \bar{J}_2, \hat{\theta}_1, \hat{\theta}_2)$  in such a way that

$$\left[ \frac{\partial \hat{H}_0}{\partial \bar{J}_2} \frac{\partial S}{\partial \hat{\theta}_2} + \{ \hat{H}_1 \} \right] = 0. \quad (37)$$

Note that this is the only term in (36) that contains the angle  $\bar{\theta}_2$ . From the equation (37) we obtain the function  $S$  as

$$S = -\frac{1}{n_2} \hat{H}_{11}(\bar{J}_1, \bar{J}_2) \frac{r}{2s-r} \sin(\bar{\theta}_1 + \frac{2s-r}{r} \bar{\theta}_2). \quad (38)$$

Then the Hamiltonian (36) takes the form, using the expression (35), to first order terms in  $\varepsilon$ ,

$$\bar{H} = \hat{H}_0(\bar{J}_1, \bar{J}_2) + \varepsilon \hat{H}_{rs}(\hat{J}_1, \hat{J}_2) \cos(r\bar{\theta}_1), \quad (39)$$

which contains only the angle  $\bar{\theta}_1$ . This means that by making use of the transformation  $\hat{J}, \hat{\theta} \rightarrow \bar{J}, \bar{\theta}$ , we generated an ignorable coordinate, the angle  $\bar{\theta}_2$ , and consequently the action  $\bar{J}_2$  is constant (in this approximation). Thus, the Hamiltonian (39) describes a system with one degree of freedom. This Hamiltonian is the *averaged Hamiltonian*.

The study of the evolution of the averaged system can be made either in the action-angle variables  $\bar{J}_1, \bar{\theta}_1$ , or in the Poincaré variables  $X = \sqrt{2\bar{J}_1} \cos \bar{\theta}_1$ ,  $Y = \sqrt{2\bar{J}_1} \sin \bar{\theta}_1$ .

The differential equations of the averaged system at the  $s/r$  resonance

From the averaged Hamiltonian (39) we obtain the differential equations of motion

$$\left. \begin{aligned} \dot{\bar{J}}_1 &= \varepsilon r \hat{H}_{rs}(\bar{J}_1, \bar{J}_2) \sin(r\bar{\theta}_1) \\ \dot{\bar{\theta}}_1 &= \frac{\partial \hat{H}_0}{\partial \bar{J}_1} + \varepsilon \frac{\partial \hat{H}_{rs}}{\partial \bar{J}_1} \cos(r\bar{\theta}_1) \end{aligned} \right\}, \quad (40)$$

and

$$\left. \begin{aligned} \dot{\bar{J}}_2 &= \frac{\partial \hat{H}_0}{\partial \bar{\theta}_2} = 0, \rightarrow \bar{J}_2 = \bar{J}_{20} \\ \dot{\bar{\theta}}_2 &= \frac{\partial \hat{H}_0}{\partial \bar{J}_2} + \varepsilon \frac{\partial \hat{H}_{rs}}{\partial \bar{J}_2} \cos(r\bar{\theta}_1) \end{aligned} \right\}. \quad (41)$$

We note that the first two equations (40) are independent of the other two equations (41). The two equations (40) describe the motion of a one degree of freedom system in the  $\bar{J}_1, \bar{\theta}_1$  variables. The action  $\bar{J}_2$  is constant, as is clear from the equations (41).

The fixed points of the averaged system at the  $s/r$  resonance

We shall study now the fixed points of the averaged equations (40). The fixed points are obtained from the equations

$$\dot{\bar{J}}_1 = 0, \quad \dot{\bar{\theta}}_1 = 0$$

and are

$$\dot{\bar{J}}_1 = 0 \rightarrow \bar{\theta}_{10} = k \frac{\pi}{r}, \quad (k = 0, 1, 2, \dots, 2r - 1), \quad (42)$$

and

$$\dot{\bar{\theta}}_1 = 0 \rightarrow \frac{\partial \hat{H}_0}{\partial \bar{J}_1} + \varepsilon \frac{\partial \hat{H}_{rs}}{\partial \bar{J}_1} \cos(r\bar{\theta}_{10}) = 0. \quad (43)$$

The equations (42) give the angles and the equation (43) gives the action  $\bar{J}_{10}$ . In addition, the action  $\bar{J}_{20}$  should correspond to the  $r/s$  resonance and the angle  $\bar{\theta}_2$  is given by

$$\bar{\theta}_2 = \bar{n}_{20}t + \bar{\theta}_{20}. \quad (44)$$

From equations (42) we see that there are  $2r$  fixed points, which belong to two groups,  $k$  even and  $k$  odd, of  $r$ - multiple fixed points:

$$k : \text{even} \rightarrow \cos(r\bar{\theta}_{10}) = +1, \quad (\bar{\theta}_{10} = \frac{2k}{r}\pi, \quad k = 0, 1, 2, \dots, r - 1). \quad (45)$$

$$k : \text{odd} \rightarrow \cos(r\bar{\theta}_{10}) = -1, \quad (\bar{\theta}_{10} = \frac{2k+1}{r}\pi, \quad k = 0, 1, 2, \dots, r - 1). \quad (46)$$

For each group of  $r$ -multiple fixed points, (42) or (43), the value of  $\bar{J}_{10}$  is the same, as we can see from (43). We shall prove in the following that each group of  $r$ -multiple fixed points corresponds to the *same* periodic orbit. Consequently, we have two  $r$ -multiple fixed points. We shall also prove that one of them is stable and the other is unstable. Note that this result is equivalent



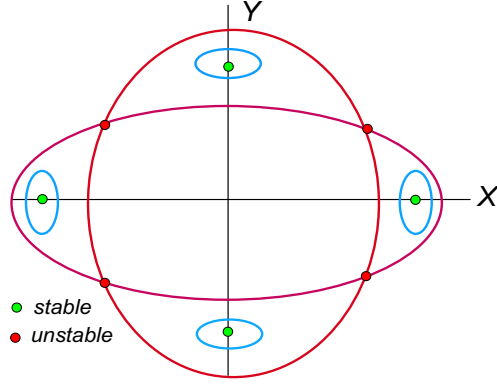


Figure 4: The phase portrait of the averaged system at the  $r/s$  resonance, for  $r = 4$  (schematically).

to the *Poincaré-Birkhoff fixed-point theorem*, mentioned in section 2. (See also Hadjidemetriou 1991). It is interesting to note from Eqs.(40) that for  $\varepsilon = 0$  the number of  $s/r$  resonant fixed points is infinite. All these fixed points lie on the level curve  $\bar{J}_1 = \bar{J}_{10}$ , for arbitrary angle  $\bar{\theta}_{10}$ . As soon as the perturbation is applied,  $\varepsilon \neq 0$ , out of this infinite set of fixed points only a finite number survives.

The evolution of the system can be studied in the  $XY$  plane,

$$X = \sqrt{2\bar{J}_1} \cos \bar{\theta}_1, \quad Y = \sqrt{2\bar{J}_1} \sin \bar{\theta}_1,$$

of the Poincaré variables. In Figure 4 we show, schematically, the phase portrait in the averaged system, close to the  $r/s$  resonance, for  $r = 4$ . There are two sets of 4-multiple fixed points, where one of them is stable and the other is unstable. Compare this with the Poincaré map, shown in Figure 3b. Although the topology in these two figures is the same, there is a great difference between these two models. In the averaged model the stable fixed points are surrounded by *level curves*, while in the Poincaré map of the non averaged model we have *invariant curves*. The difference, (level curves in the averaged system and invariant curves in the non averaged system) is due to the fact that the non averaged system has two degrees of freedom, while the averaged system (equations (40)) has only one degree of freedom. Thus, the averaged system is integrable and the motion is ordered, while in the non averaged system chaos may appear, starting from the vicinity of the unstable fixed points, as we shall show in the following.

*The relation of the solution of the averaged system with the solution of the non averaged system*

We shall find now the relation between the solution of the averaged system (39) with the solution of the non averaged system (21). This is given by the canonical transformation from the averaged variables  $\bar{J}_1, \bar{J}_2, \bar{\theta}_1, \bar{\theta}_2$  to the original action-angle variables  $J_1, J_2, \theta_1, \theta_2$ . These transformation equations are

$$\left. \begin{aligned} J_1 &= \bar{J}_1 - \frac{\varepsilon}{n_2} \frac{r}{s-r} \hat{H}_{11}(\bar{J}_1, \bar{J}_2) \cos(\bar{\theta}_1 + \frac{2s-r}{r} \bar{\theta}_2), \\ \theta_1 &= \bar{\theta}_1 + \frac{s}{r} \bar{\theta}_2 + \frac{\varepsilon}{n_2} \frac{r}{s-r} \left( \frac{\partial \hat{H}_{11}}{\partial J_1} + \frac{s}{r} \frac{\partial \hat{H}_{11}}{\partial J_2} \right) \sin(\bar{\theta}_1 + \frac{2s-r}{r} \bar{\theta}_2), \\ J_2 &= -\frac{s}{r} \bar{J}_1 + \bar{J}_2 + \frac{\varepsilon}{n_2} \frac{r}{s-r} \hat{H}_{11}(\bar{J}_1, \bar{J}_2) \cos(\bar{\theta}_1 + \frac{2s-r}{r} \bar{\theta}_2), \\ \theta_2 &= \bar{\theta}_2 + \frac{\varepsilon}{n_2} \frac{r}{s-r} \frac{\partial \hat{H}_{11}}{\partial J_2} \sin(\bar{\theta}_1 + \frac{2s-r}{r} \bar{\theta}_2). \end{aligned} \right\} \quad (47)$$

The relation between the fixed points of the averaged Hamiltonian with the periodic orbits of the non averaged system

We shall prove now that a fixed point solution of the averaged system (39), given by equations (42), (43), corresponds to a periodic solution of the non averaged system (21). Using (43), (44) and (46) we obtain from the relations (47), for a certain fixed point solution  $\bar{J}_{10}, \bar{\theta}_{10}, \bar{J}_{20}, \bar{\theta}_2 = \bar{n}_{20}t + \theta_{20}$ , the solution of the non averaged system

$$\left. \begin{aligned} J_1 &= \bar{J}_{10} - \frac{\varepsilon}{n_2} \frac{r}{s-r} \hat{H}_{11}(\bar{J}_{10}, \bar{J}_{20}) \cos(\bar{\theta}_{10} + \frac{2s-r}{r} \bar{n}_{20}t), \\ \theta_1 &= \bar{\theta}_{10} + \frac{s}{r} \bar{n}_{20}t + \frac{\varepsilon}{n_2} \frac{r}{s-r} \left( \frac{\partial \hat{H}_{11}}{\partial J_{10}} + \frac{s}{r} \frac{\partial \hat{H}_{11}}{\partial J_{20}} \right) \sin(\bar{\theta}_{10} + \frac{2s-r}{r} \bar{n}_{20}t), \\ J_2 &= -\frac{s}{r} \bar{J}_{10} + \bar{J}_{20} + \frac{\varepsilon}{n_2} \frac{r}{s-r} \hat{H}_{11}(\bar{J}_{10}, \bar{J}_{20}) \cos(\bar{\theta}_{10} + \frac{2s-r}{r} \bar{n}_{20}t), \\ \theta_2 &= \bar{\theta}_{20} + \bar{n}_{20}t + \frac{\varepsilon}{n_2} \frac{r}{s-r} \frac{\partial \hat{H}_{11}}{\partial J_{20}} \sin(\bar{\theta}_{10} + \frac{2s-r}{r} \bar{n}_{20}t). \end{aligned} \right\} \quad (48)$$

From equations (48) we see that a certain fixed point solution of the averaged system corresponds to a *periodic solution* of the non averaged system, with period

$$T = \frac{2\pi}{\bar{n}_{20}} r.$$

During one period  $T$ , the angle  $\theta_1$  makes  $s$  revolutions (increases by  $2\pi s$ ) and the angle  $\theta_2$  makes  $r$  revolutions (increases by  $2\pi r$ ).

We shall prove now that the above periodic solution is an  $r$ -multiple periodic solution. To do so, we take the Poincaré map of the periodic solution (48) on the surface of section (8), i.e. at  $\theta_2 = 0$ , and we see that it is represented by an  $r$ -multiple fixed point. This is so, because we have  $r$  intersections with the circle  $\theta_2 = 0$  before we come to the initial point. The consecutive points of intersection at  $\theta_2 = 0$  are at the times  $t = (2\pi/n_{20})\nu$ ,  $\nu = 0, 1, 2, \dots, r-1$ , to zero order terms in  $\varepsilon$  (the exact times of intersection are slightly different). The angle  $\theta_1$  advances at each intersection by  $2\pi s/r$ , to zero order terms in  $\varepsilon$ .

Next, we shall prove that the above points of intersection of the Poincaré map correspond to the fixed points (45) or (46) of the averaged Hamiltonian. This is so, because if we start the periodic solution (48) from a certain fixed point (45) or (46), the next fixed point of the Poincaré map of the solution (48), as defined above at  $\theta_2 = 0$ , is a point of the *same* set (45) or (46) (prove it!). This means that each set of fixed points (45) and (46) corresponds to the *same*  $r$ -multiple periodic orbit. Consequently, *to an  $r$ -multiple fixed point of the averaged system, there corresponds a single  $r$ -multiple periodic orbit of the non averaged system*. Since there are two  $r$ -multiple fixed points of the averaged Hamiltonian, there are two  $r$ -multiple periodic solutions of the non averaged Hamiltonian. In the next section we will prove that one of these orbits is stable and the other is unstable.

Stability

We shall study now the stability of the periodic orbits, in the variables  $\theta_1, \theta_2, J_1, J_2$ , given by the relations (48). The stability is the same as the stability of the fixed points of the system (40), (41), in the variables  $\bar{\theta}_1, \bar{\theta}_2, \bar{J}_1, \bar{J}_2$ . Note that these two sets of variables are related by a canonical transformation, which conserves the stability indices.

We shall study the stability using the system (40), (41), considering it as representing a system with two degrees of freedom, as is the case with the system (48). For reasons of brevity, we

define the functions

$$g(\bar{J}) = \hat{H}_{rs}, \quad f_i(\bar{J}) = \frac{\partial}{\partial \bar{J}_i}(\hat{H}_0 + \varepsilon \hat{H}_{00}), \quad g_i(\bar{J}) = \frac{\partial \hat{H}_{rs}}{\partial \bar{J}_i}, \quad i = 1, 2.$$

Then the system (40), (41) takes the form

$$\begin{aligned} \dot{\bar{\theta}}_1 &= f_1(\bar{J}) + \varepsilon g_1(\bar{J}) \cos(r\theta_1), \\ \dot{\bar{J}}_1 &= \varepsilon r g_1(\bar{J}) \sin(r\theta_1), \\ \dot{\bar{\theta}}_2 &= f_2(\bar{J}) + \varepsilon g_2(\bar{J}) \cos(r\theta_1), \\ \dot{\bar{J}}_2 &= 0. \end{aligned}$$

The fixed point solution (42)-(44) takes the form

$$\bar{J}_{10}, \quad \bar{\theta}_{10} = k\pi/r, \quad \bar{J}_{20}, \quad \bar{\theta}_2 = \bar{n}_{20}t + \bar{\theta}_{20},$$

and the corresponding system of variational equations are

$$\dot{\xi} = A\xi,$$

where the column vector  $\xi$  is defined as

$$\xi = (\Delta \bar{\theta}_1, \Delta \bar{J}_1, \Delta \bar{\theta}_2 - \bar{n}_{20}t, \Delta \bar{J}_2)^t,$$

the superscript  $t$  meaning transpose, and the matrix  $A$  is given by

$$\begin{pmatrix} 0 & \alpha_1 & 0 & \alpha_2 \\ \gamma & 0 & 0 & 0 \\ 0 & \beta_1 & 0 & \beta_2 \\ 0 & 0 & 0 & 0 \end{pmatrix},$$

where

$$\gamma = \varepsilon r^2 g_0 c_0, \quad \alpha_i = \frac{\partial}{\partial \bar{J}_i}(f_1 + \varepsilon g_1 c_0), \quad \beta_i = \frac{\partial}{\partial \bar{J}_i}(f_2 + \varepsilon g_2 c_0),$$

and we have abbreviated

$$c_0 \equiv \cos(r\bar{\theta}_{10}) = \cos(k\pi).$$

The eigenvalues of the matrix  $A$  are

$$\lambda_{1,2} = \pm \sqrt{\alpha_1 \gamma}, \quad \lambda_3 = \lambda_4 = 0.$$

Since  $\gamma = \varepsilon r^2 g_0 \cos(k\pi)$ , we come to the conclusion that one set of fixed points (45), for  $k = \text{even}$ , corresponds to  $\gamma > 0$  and the other set of fixed points (46), for  $k = \text{odd}$ , corresponds to  $\gamma < 0$ . Consequently, we come to the conclusion that *one of the above sets of fixed points is stable ( $\lambda_{1,2}$ : imaginary) and the other set is unstable ( $\lambda_{1,2}$ : real), depending on the sign of  $\alpha_1$ .*

Note that the existence of the two zero eigenvalues  $\lambda_3 = \lambda_4 = 0$  is due to the fact that the system (40), (41), obtained from the averaged Hamiltonian (39), has the energy integral  $\bar{H} = \text{constant}$ .

#### Comparison between the Poincaré map and the averaged Hamiltonian

We remark at this point that the Poincaré map represents accurately the dynamical system (4), while the method of averaging is an approximate method, because the averaged Hamiltonian

(39) is obtained by a perturbation method, and in fact, this latter Hamiltonian is a first order approximation. But even in higher order approximations, the averaged Hamiltonian does not represent always the original, non averaged, system, because the perturbation series, in general, do not converge. This is always the case in non integrable systems. So, the phase portrait of the Poincaré map of the original system may be different from the phase portrait of the corresponding averaged system. In general, these two phase portraits may coincide in those regions of the phase space where the system behaves as integrable, i.e. there exist smooth invariant curves. If chaos appears, then the method of averaging is not applicable. These will be explained in the next section, by an example. Thus we come to the conclusion that *a necessary criterion for the averaged model to be realistic is, the fixed points of the averaged Hamiltonian to coincide with the periodic orbits / fixed points of the Poincaré map of the original system.*

## 4 An example

We shall present now an example to make clear the results of the previous two sections. Let us consider a dynamical system defined by the Hamiltonian

$$H = J_1^2 + 3J_1 + 2J_2^2 + \varepsilon J_1 J_2 \cos(2\theta_1 - \theta_2) + \varepsilon J_1 J_2^{3/2} \cos(2\theta_1 - 3\theta_2). \quad (49)$$

The part

$$H_0 = J_1^2 + 3J_1 + 2J_2^2 \quad (50)$$

in the right hand side of (49) is the integrable part. This is a system with two degrees of freedom, in the variables  $J_1, J_2, \theta_1, \theta_2$ , which are the action-angle variables of the integrable part (50) of the Hamiltonian (49). The frequencies of the integrable Hamiltonian are

$$n_1 = \frac{\partial H}{\partial J_1} = 2J_1 + 3, \quad n_2 = \frac{\partial H}{\partial J_2} = 4J_2, \quad (n_1 = \dot{\theta}_1, n_2 = \dot{\theta}_2).$$

Note that there are two basic frequencies in (49),

$$n_1/n_2 = 1/2, \quad n_1/n_2 = 3/2. \quad (51)$$

The initial conditions corresponding to these frequencies, in the actions  $J_1, J_2$  (and arbitrary angles  $\theta_1, \theta_2$ ), are

$$\frac{n_1}{n_2} = \frac{2J_1 + 3}{4J_2} = \frac{1}{2} \rightarrow J_2 = J_1 + \frac{3}{2}, \quad (52)$$

for the 1/2 resonance and

$$\frac{n_1}{n_2} = \frac{2J_1 + 3}{4J_2} = \frac{3}{2} \rightarrow J_2 = \frac{1}{3}J_1 + \frac{1}{2}, \quad (53)$$

for the 3/2 resonance. The resonance curves, for the above two frequencies, in the space  $J_1, J_2$ , are given in Figure 5a.

### The Poincaré map

We consider the Poincaré map of the system (49) for the surface of section

$$h = 10, \quad \theta_2 = 0. \quad (54)$$

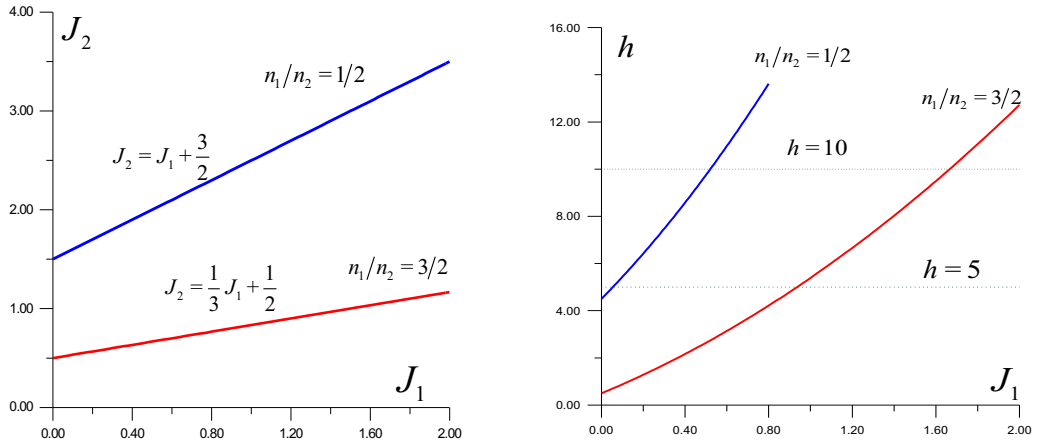


Figure 5: The resonance curves, for the basic resonances  $1/2$  and  $3/2$  in the action space . (b) The energy curves, in the space  $J_1, h$ .

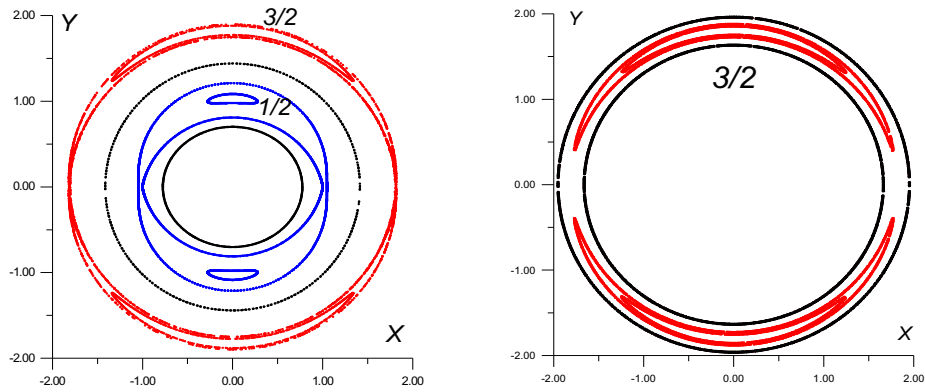


Figure 6: Perturbation  $\varepsilon = 0.03$ . (a) The Poincaré map of the system (49). Both resonances  $1/2$  and  $3/2$  are present. The invariant curves are smooth. (b) The level curves of the averaged Hamiltonian close to the  $3/2$  resonance.

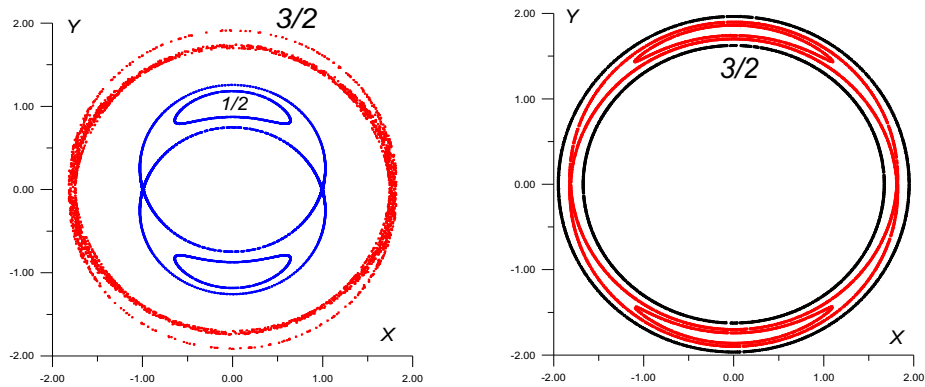


Figure 7: Perturbation  $\varepsilon = 0.05$ . (a) The Poincaré map of the system (49). Both resonances  $1/2$  and  $3/2$  are present. Chaotic motion starts at the unstable fixed points at the  $3/2$  resonance. (b) The level curves of the averaged Hamiltonian close to the  $3/2$  resonance.

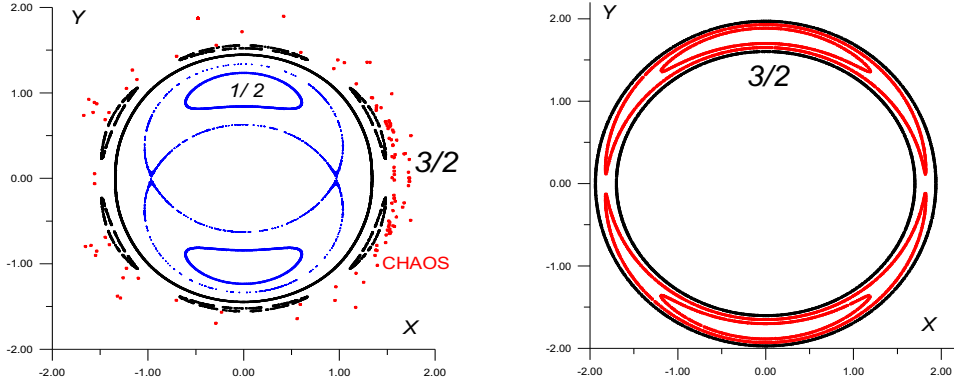


Figure 8: Perturbation  $\varepsilon = 0.10$ . (a) The Poincaré map of the system (49). Both resonances 1/2 and 3/2 are present. In addition, higher order resonances also appear. There is extended chaotic motion at the 3/2 resonance. (b) The level curves of the averaged Hamiltonian close to the 3/2 resonance.

Let us assume, as a first approximation, that the energy  $h$  is a function of the unperturbed Hamiltonian (50),  $h = H_0(J_1, J_2)$ . By making use of the relations (52), (53) between the actions  $J_1, J_2$ , along the resonances 1/2 and 3/2, respectively, we find the energy curves, in the space  $J_1 h$ , for these two resonances, as shown in Figure 5b. From this diagram we can find, to a first approximation, the value of the action  $J_1$  for the resonances 1/2 and 3/2, for any energy level.

We shall compute the Poincaré map for the surface of section (54), at the energy level  $h = 10$ . We shall use the complete system (49). In order to select the initial conditions close to the 1/2 and 3/2 resonances, we shall use the analysis of the unperturbed Hamiltonian (50). From Figure 5b and using also equation (53) we find that at this energy level it is  $J_1 \approx 0.5, J_2 \approx 1.25$ , for the 1/2 resonance and  $J_1 \approx 1.6, J_2 \approx 1.1$  for the 3/2 resonance. In the Figures 6a, 7a and 8a we present the Poincaré maps for the whole space in the Poincaré variables  $X = \sqrt{2J_1} \cos \theta_1, Y = \sqrt{2J_1} \sin \theta_1$ , for increasing values of the perturbation,  $\varepsilon = 0.03, \varepsilon = 0.05, \varepsilon = 0.10$ , respectively. Both resonances appear and, in addition, for the case of the larger perturbation  $\varepsilon = 0.10$ , higher order resonances also appear, due to the nonlinearity of the system. Note that the position of the fixed points in the Poincaré diagrams coincide with the intersection of the resonance curve with the line  $h = 0.10$  in Figure 5b.

#### The level curves of the averaged Hamiltonian

We shall work in the region of the 3/2 resonance. The resonance variables, as obtained from the relations (28) are

$$\left. \begin{aligned} \hat{J}_1 &= J_1, & \hat{J}_2 &= \frac{3}{2}J_1 + J_2, \\ \hat{\theta}_1 &= \theta_1 - \frac{3}{2}\theta_2, & \hat{\theta}_2 &= \theta_2, \end{aligned} \right\} \quad (55)$$

and it is easily seen that the angle  $\theta_1$  is a ‘slow’ angle, because  $\dot{\hat{\theta}}_1$  is small at the 3/2 resonance. The averaged Hamiltonian, as obtained from (49), is

$$\bar{H} = \bar{J}_1^2 + 3\bar{J}_1 + 2 \left( -\frac{3}{2}\bar{J}_1 + \bar{J}_2 \right)^2 + \varepsilon \bar{J}_1 \left( -\frac{3}{2}\bar{J}_1 + \bar{J}_2 \right)^{3/2} \cos(2\bar{\theta}_1), \quad (56)$$

in the variables  $\bar{J}_1, \bar{\theta}_1$ . The angle  $\bar{\theta}_2$  is ignorable and consequently the action  $\bar{J}_2$  is constant. This is an approximate integral of motion, and in zero order terms is given by

$$\bar{J}_{20} \approx \frac{3}{2}J_1 + J_2. \quad (57)$$

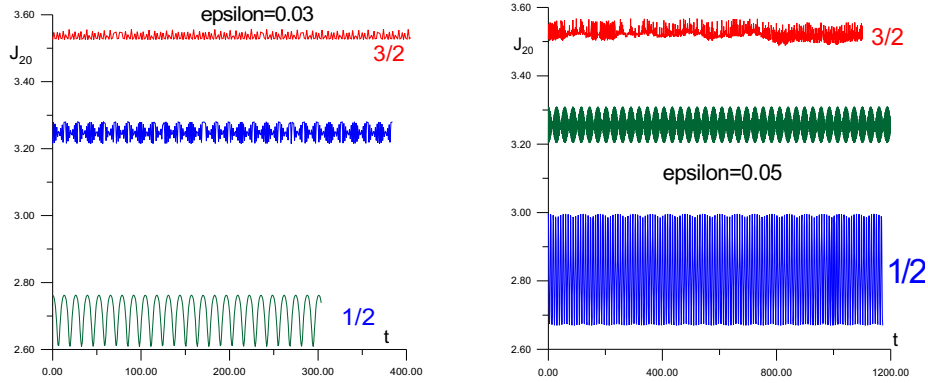


Figure 9: The approximate integral  $\bar{J}_{20}$  at the  $3/2$  resonance and at the  $1/2$  resonance and far from resonance, for  $\varepsilon = 0.03$ . (b) The approximate integral  $\bar{J}_{20}$  at the  $3/2$  resonance and at the  $1/2$  resonance and far from resonance, for  $\varepsilon = 0.05$ .

The level curves of the averaged Hamiltonian (56) describe the evolution of the system, in the  $\bar{J}_1, \bar{\theta}_1$  variables. Since  $\bar{J}_2$  is constant, this latter Hamiltonian is equivalent to a system with one degree of freedom. The parameter for each phase portrait of the level curves is the value of the action  $\bar{J}_2$ , which is constant. Note that in the phase space of the Poincaré map the parameter was the energy  $h$ .

In Figures 6b, 7b and 8b we present the level curves of the averaged Hamiltonian (56), for the perturbation  $\varepsilon = 0.03$ ,  $\varepsilon = 0.05$ ,  $\varepsilon = 0.10$ , respectively. The value of the parameter  $\bar{J}_2$  is selected in such a way in order to correspond to the energy level  $h = 10$  of the Poincaré map presented in Figures 6a, 7a and 8a. From the values  $J_1 \approx 1.6$  and  $J_2 \approx 1.1$  that correspond to the  $3/2$  resonance, and using relations (55), we find  $\bar{J}_{20} = 3.5$ . We also remark that the Poincaré variables  $X = \sqrt{2J_1} \cos \theta_1$ ,  $Y = \sqrt{2J_1} \sin \theta_1$  used in the mapping of the Figures 6a, 7a and 8a are equivalent, to first order terms in  $\varepsilon$ , to the Poincaré variables in the averaged action-angles  $X = \sqrt{2\bar{J}_1} \cos \bar{\theta}_1$ ,  $Y = \sqrt{2\bar{J}_1} \sin \bar{\theta}_1$ , as can be seen from the transformation equations (55), taking also into account that  $\theta_2 = 0$  on the Poincaré map.

A first remark from the comparison of the figures 6a - 6b, 7a - 7b and 8a - 8b, is that there is a similarity in the topology, in the sense that the position and the stability character of the fixed points of the  $3/2$  resonance is the same. However, the level curves of the averaged Hamiltonian are smooth curves, implying that the motion is ordered everywhere, since the one degree of freedom averaged model is integrable. On the contrary, the invariant curves of the Poincaré map are smooth curves only for a small perturbation, as seen from the comparison between the Figures 6a and 6b. For a larger perturbation,  $\varepsilon = 0.05$ , the invariant curves start to dissolve at the unstable fixed points, and for a still larger perturbation,  $\varepsilon = 0.10$ , there is widespread chaos at the whole region of the  $3/2$  resonance. We also remark that the averaged model (56) is valid only close to the  $3/2$  resonance, and for this reason in the level curves the resonance  $1/2$  does not appear.

It is also interesting to see the properties of the approximate integral  $\bar{J}_{20} \approx \frac{3}{2}J_1 + J_2 = \text{constant}$ . In Figures 9a and 9b we plot the value of  $\bar{J}_{20}$  close to the  $3/2$  resonance and far from this resonance. It is clear, even in the zero order approximation that we use here, that the variation of  $\bar{J}_{20}$  is much smaller close to the  $3/2$  resonance than far from it.

## 5 Discussion

The Poincaré map and the method of averaging are two useful methods that are used in the study of the dynamics and the evolution of a dynamical system. Each method has its advantages and disadvantages. The Poincaré map describes accurately the dynamical system, but is a purely numerical method, with all the advantages and the limitations of a numerical work. On the other hand, the method of averaging is an analytic method, and one can understand better the dynamics of the system. However, it is based on a perturbation method, involving series expansions in powers of a small parameter. Unfortunately, these series do not converge (they are asymptotic series) and in many cases the dynamical system that the averaged system describes may be different from the real system. In such cases the inclusion of higher order terms does not improve the situation, and there may be an optimal order, beyond which things deteriorate. This is the rule in a non integrable dynamical system, but this does not mean that the method of averaging is not applicable in these cases. In the regions of the phase space where the system behaves as integrable (smooth invariant curves), the averaged model may give important information on the dynamics. This is clearly seen from the example of the system (49), as shown in Figures 7, 8 and 9.

We believe that both methods are useful and complementary in the study of a dynamical system, and both of them should be used. Note that a necessary condition for the averaged model to be realistic is to have the same fixed points, with the same stability character, as the Poincaré map. This is necessary in order for the topology of the averaged model to coincide with the topology of the real system, as presented by the Poincaré map, since it is the fixed points that determine the topology of the phase space.

## References

- [1] Arnold V.A. (1978): *Mathematical Methods of Classical mechanics*, Springer-Verlag.
- [2] Arnold, V.A., Avez, A. (1968): *Ergodic Problems of Classical Mechanics*, W.A.Benjamin, New York.
- [3] Hadjidemetriou, J.D. (1998): *Symplectic Maps and their use in Celestial Mechanics*, in D. Benest and C. Froeschlé (eds.) *Analysis and Modeling of Discrete Dynamical Systems*, chapter 9, pp 249-282, Gordon and Breach Publ.
- [4] Hadjidemetriou, J.D. (1991): *Mapping Models for Hamiltonian Systems with application to Resonant Asteroid Motion*, in A.E. Roy (ed.) *Predictability, Stability and Chaos in N-Body Dynamical Systems*, Plenum Press.
- [5] Lichtenberg, A.J. and Liebermann, M.A. (1983): *Regular and Stochastic Motion*, Springer-Verlag.